

DOI: 10.1002/cphc.201402057

# Slide Fastener Reduction of Graphene-Oxide Edges by Calcium: Insight from Ab Initio Molecular Dynamics

Sheng-Yi Xie,<sup>[a]</sup> Xian-Bin Li,<sup>\*[a]</sup> Wei Quan Tian,<sup>[a, b]</sup> Dan Wang,<sup>[a]</sup> Nian-Ke Chen,<sup>[a]</sup> Dong Han,<sup>[a]</sup> and Hong-Bo Sun<sup>\*[a, c]</sup>

The reduction of graphene oxide can be used as a simple way to produce graphene on a large scale. However, the numerous edges produced by the oxidation of graphite seriously degrade the quality of the graphene and its carrier transport property. In this work, the reduction of oxygen-passivated graphene edges and the subsequent linking of separated graphene sheets by calcium are investigated by using first-principles calculations. The calculations show that calcium can effectively remove the oxygen groups from two adjacent edges. The join-

ing point of the edges serves as the starting point of the reduction and facilitates the reaction. Once the oxygen groups are removed, the crack is sutured. If the joining point is lacking, it becomes difficult to zip the separated fragments. A general electron-reduction model and a random atom-reduction model are suggested for these two situations. The present study sheds light on the reduction of graphene-oxide edges by using reactive metals to give large-sized graphene through a simple chemical reaction.

## 1. Introduction

Graphene holds great promise for the next generation of nanoscience and nanotechnology.<sup>[1–4]</sup> However, the large-scale production of graphene in high yield and at low cost is a bottleneck for basic research or industrial applications. The reduction of graphene oxide (GO) could potentially solve the yield and cost difficulties.<sup>[5,6]</sup> GO is produced by the oxidation of graphite. Through the attack of oxygen, the C–C bond can be broken to form exfoliated GO fragments from graphite.<sup>[7,8]</sup> Experimental<sup>[9–11]</sup> and theoretical studies<sup>[12–14]</sup> have revealed the progress of the oxidation; for example, Fujii and Enoki suggested the use of an atomic force microscopy (AFM) probe as a tool to cut the oxidized graphene into pieces.<sup>[10]</sup> From a theoretical viewpoint, Ma et al. demonstrated that strain can induce orientation-selective cutting of graphene by oxidation.<sup>[14]</sup> These oxidations need precise control. However, the quality of graphene produced by using common oxidation techniques is low, because the oxidation process damages the graphene lattice and produces cracks or edges. This is the

main demerit of this method. Meanwhile, the oxygen groups adhere strongly to the edges of the graphene and are hardly removed during the reduction process.<sup>[15]</sup> To solve this problem, many methods have been developed; for example, high-temperature heating<sup>[16]</sup> as well as hydrazine,<sup>[17]</sup> hydrogen,<sup>[18]</sup> NaBH<sub>4</sub>,<sup>[19]</sup> HI,<sup>[20]</sup> and laser reduction.<sup>[21]</sup> However, these methods are not efficient enough to reduce the stable oxygen groups at the edges. Metals such as Fe,<sup>[22]</sup> Zn,<sup>[23]</sup> and alkaline-earth metals<sup>[24]</sup> provide alternative ways to reduce GO effectively and rapidly. These metals have a high reduction potential and are able to remove the oxygen atoms from the central part of the sheet. Can metals also effectively reduce the stable oxygen groups at the GO edges?

In this work, we study the reduction of GO edges by the alkaline-earth metal calcium (Ca) using ab initio molecular dynamic (AIMD) simulations. For a crack with a carbon (C)-atom joint, named a partially torn GO edge (PT-edge) in this work, the reduction takes place quickly, starting at the joint position. Conversely, for a crack without a C-atom joint, termed a completely torn GO edge (CT-edge), the reduction proceeds very slowly. The delocalized lowest unoccupied orbital of the PT-edge can accept electrons from the distant Ca atom, which makes the reduction fast and effective. The joint C atom of the PT-edge acts as a zipper to facilitate the reduction. However, the localized lowest unoccupied orbital of the CT-edge suppresses the electron transfer from the distant Ca atom. The reduction of the CT-edge depends on the random movement of Ca atoms close to the carbonyl groups. The present work reveals that Ca can remove the oxygen groups and partially integrate GO fragments.

[a] S.-Y. Xie, Dr. X.-B. Li, Prof. W. Q. Tian, D. Wang, N.-K. Chen, D. Han, Prof. H.-B. Sun

State Key Laboratory on Integrated Optoelectronics  
College of Electronic Science and Engineering, Jilin University  
2699 Qianjin Street, Changchun 130012 (PR China)  
Fax: (+86)431 85168281  
E-mail: lixianbin@jlu.edu.cn  
hbsun@jlu.edu.cn

[b] Prof. W. Q. Tian

Institute of Theoretical Chemistry, Jilin University  
2699 Qianjin Street, Changchun 130012 (PR China)

[c] Prof. H.-B. Sun

College of Physics, Jilin University  
2699 Qianjin Street, Changchun 130012 (PR China)

 Supporting Information for this article is available on the WWW under <http://dx.doi.org/10.1002/cphc.201402057>.

## Computational Methods

AIMD calculations were carried out with the Vienna ab initio simulation package (VASP) code.<sup>[25]</sup> The projector augmented wave (PAW)<sup>[26]</sup> method was used to describe the interaction of the core and valence electrons. The generalized gradient approximation of Perdew, Burke, and Ernzerhof (PBE)<sup>[27]</sup> was taken for electron exchange and correlation. GO was taken to be a 32-carbon graphene unit cell, with carbonyl groups at its edges (as shown in Figure 1). The time step was chosen as 1 fs, and the canonical ensemble was employed, in which the number of atoms, the volume, and the temperature (NVT) were set as the thermodynamic variables of the system. The Nosé–Hoover thermostat was used to control the temperature of the system.<sup>[28]</sup> Brillouin-zone sampling was only taken at the  $\Gamma$  point for AIMD; larger  $k$  mesh calculations were tested and gave the same results (Figure S1 in the Supporting Information). The energy cutoff of the plane-wave basis sets was 400 eV. The AIMD simulations for reduction were carried out in two steps. First, the system temperature was increased from 0 to 600 K in 1 ps, and the system temperature was then kept constant at 600 K for tens of picoseconds. Two models for the AIMD simulation are discussed in the following section.

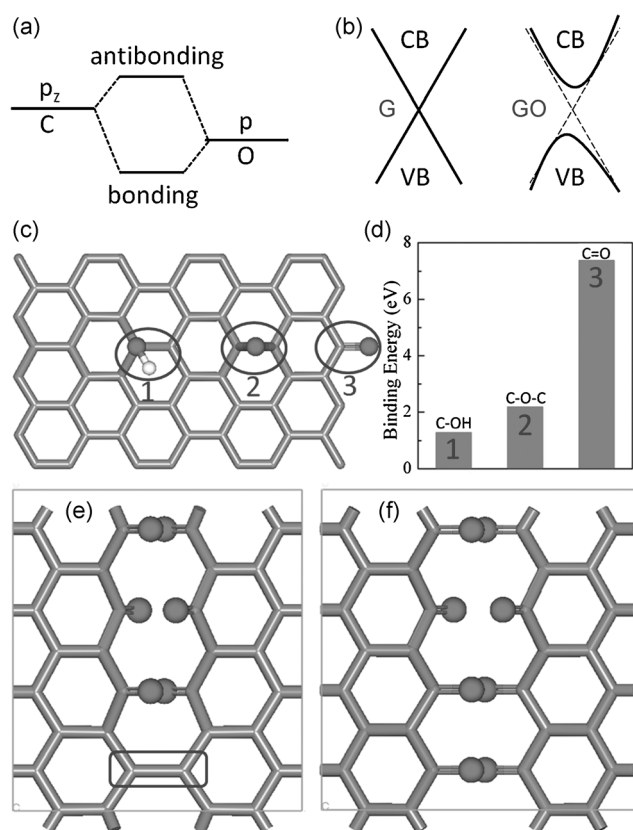


**Figure 1.** a) Bonding between C and O atoms; b) sketch of valence band (VB) and conduction band (CB) for graphene and GO; c) GO with internal oxygen groups: hydroxyl (C–OH), epoxide (C–O–C), and edge carbonyl (C=O), marked as 1, 2, and 3 with dark-grey ellipses; d) binding energy of oxygen groups; e) PT-edge; and f) CT-edge GO models. The rectangle in (e) indicates the joint position in the PT-edge model. Grey and white spheres represent oxygen and hydrogen, respectively; grey sticks are carbon.

## 2. Results and Discussion

## 2.1. Oxygen at Graphene Edges

The essence of oxidation in graphene is the bonding of the  $p_z$  orbital of the C atom with the p orbital of the O atom, as shown in Figure 1a and b. Li et al. demonstrated that the cooperative alignment of epoxides can break the C–C bond.<sup>[7]</sup> Further, Li et al. pointed out that ordered epoxide pairs with one above and one below the sheet will eventually evolve into carbonyl pairs and tear the graphene with a small barrier.<sup>[8]</sup> By this means, cracks or edges emerge during the oxidation. Edges have a different chemical environment to the inside of the sheet. C atoms inside the sheet bind three neighboring C atoms, whereas C atoms located at the edges bind only two neighboring C atoms. The absence of one C–C bond changes the chemical properties of C at the edges. Inside the graphene sheet, O binds to C with a single O–C bond, forming, for example, epoxide (C–O–C) or hydroxyl (C–OH) groups. However, groups with a double C=O bond, for example, carbonyl (C=O), form at the edges.<sup>[15]</sup> It is difficult to reduce the oxygen groups at the edges because of their large binding energy. The binding energy of carbonyl is 7.32 eV, which is far larger than that of epoxide (2.19 eV) and hydroxyl (1.29 eV), as shown in Figure 1c and d. Traditional reduction methods, such as thermal reduction, cannot break the C=O bond of the carbonyl group, and CO is likely to be the product at high temperatures.<sup>[16]</sup> For commonly used reduction agents, for example,  $N_2H_4$ ,  $H_2$ ,  $NaBH_4$ , and HI, the key to reduction depends on the bonding of hydrogen to the oxygen groups.<sup>[29]</sup> However, the reduction ability of hydrogen is limited due to its ionization energy of 13.6 eV, which is much larger than that of metal Ca: 6.1 eV.<sup>[30]</sup> The ionization energy describes the minimum energy required to remove an electron from an atom. To reduce the stable carbonyls at the edge, Ca could be a better reduction agent. Ca has been widely used for reducing metals from their oxides, such as  $ZrO_2$ <sup>[31]</sup> and  $TiO_2$ .<sup>[32]</sup> Previous theoretical work also suggests that Ca is a good reduction agent for oxygen groups inside the sheet<sup>[24]</sup> and has the potential for industrial application due to the low cost of the raw material.

## 2.2. Two GO Edge Models

To check the reduction ability of Ca for carbonyls at the edges, two types of edge models are considered in this work. 1) PT-edge model: oxidation partially damages the graphene lattice such that two edges connect at one point of the graphene lattice. This PT-edge is produced by six carbonyls orderly arranged along the edge, with one C–C pair unoxidized (Figure 1e). 2) CT-edge model: oxidation completely separates the graphene lattice. The CT-edge is obtained by the formation of eight carbonyls, which cuts the graphene completely into two fragments, as shown in Figure 1f. The Coulomb repulsion of carbonyls between the edges separates the two fragments. Before molecular dynamics simulations, the two GO edge structures are relaxed until the force is smaller than  $0.1 \text{ eV \AA}^{-1}$ .

Li et al.<sup>[8]</sup> suggested that the unzipping barrier to oxidation is as small as 0.26 eV in a perfect graphene lattice once a carbonyl pair is formed. According to this result, it is difficult for the PT-edge to survive. In fact, in previous experimental work PT-edges have been found in transmission electron microscopy (TEM) images.<sup>[33,34]</sup> This situation may result from impurities, defects, or grain boundaries that are introduced before and after oxidation, which may increase the barrier and prevent further unzipping.

### 2.3. Reduction of PT-Edges by Ca

Eight Ca atoms were placed up and down the GO sheet, with a density close to that of the Ca(001) plane. Figure 2 gives the snapshots of the reduction. At first, Ca atoms move toward the carbonyls of the GO edges. As the temperature of the system

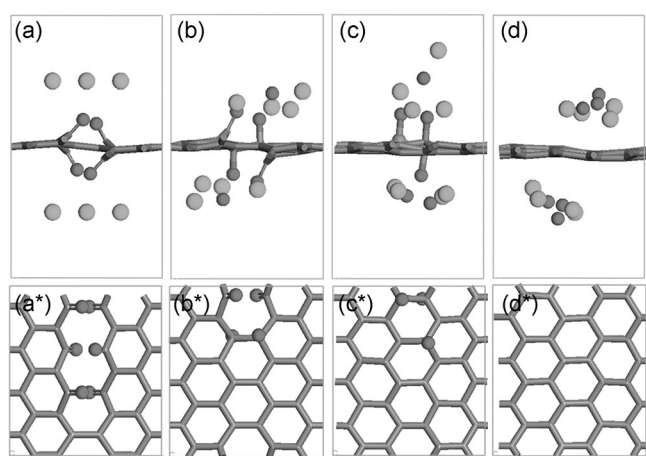


**Figure 2.** Ca reduction of a PT-edge: a) initial structure and b) snapshot during 1 ps heating from 0 to 600 K. Further snapshots were obtained after c) 2 ps and d) 6 ps annealing at 600 K. a\*–d\*) Corresponding top views of GO for (a)–(d). The slightly larger grey spheres are Ca, the smaller dark-grey spheres represent oxygen, and the grey sticks are carbon.

rises from 0 to 600 K in 1 ps, two carbonyls close to the joint are removed by Ca, as shown in Figure 2b and b\*. With the reduction of two carbonyl groups, the originally broken C–C bond is repaired. The reduction temperature is kept at 600 K, and after a further 2 ps, as shown in Figure 2c, the third carbonyl is removed. After 6 ps, all six carbonyls are completely reduced by Ca and the carbon network is repaired, as shown in Figure 2d\*. The original joint point of the two edges serves as the starting point of the reduction. Upon the reduction of the first two carbonyl groups, the broken C–C bond is healed and becomes a new joint. The reduction continues and the joint moves until all of the carbonyl oxygen atoms are removed.

### 2.4. Reduction of CT-Edge by Ca

For the CT-edge, eight Ca atoms are used to reduce eight carbonyls that are orderly arranged to form the CT-edges. Figure 3a gives the original structure before the reduction. After

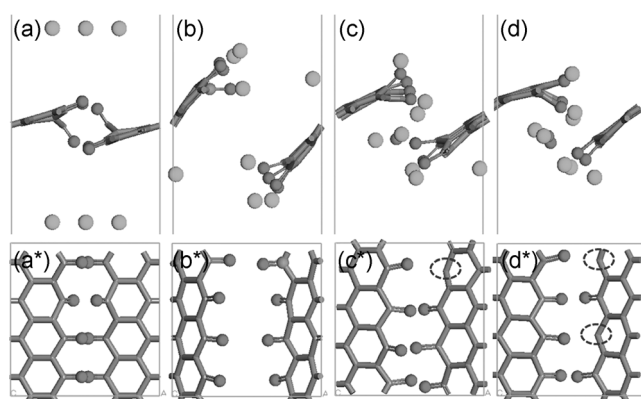


**Figure 3.** Ca reduction process for a CT-edge: a) initial structure; b) snapshot after 1 ps heating from 0 to 600 K; snapshots after annealing for c) 2 ps and d) 6 ps at 600 K. a\*–d\*) Corresponding top views of GO for (a)–(d). The dashed ellipses in (c\*) and (d\*) indicate the reduced carbon sites; other atoms are the same as in Figure 2.

the heating progresses from 0 to 600 K in 1 ps, the Ca atoms and carbonyl groups are attracted to each other and the Ca atoms move towards the carbonyls. On retaining the system temperature at 600 K for 2 ps, one carbonyl in the right-hand fragment is reduced by Ca, as shown in Figure 3c and c\*. The reduced C atom with a dangling bond becomes an active site for chemical reaction. Within a further 4 ps, another carbonyl in the right-hand fragment is reduced, as shown in Figure 3d and d\*. Although two of a total of eight carbonyls are reduced, the two fragments are still separated from each other. A further 20 ps simulation does not result in the reduction of any other new carbonyl groups. The random reductions of the C atoms are independent of each other, with little facilitation of further reduction; thus, the reduction becomes slower than the reduction of the PT-edge.

### 2.5. Slide Fastener Reduction Mechanism

The two GO edge models described above show different responses to Ca reduction. Two key factors are crucial for the reduction. 1) Structural factor: atomic topological arrangement of the GO edge strongly affects the reduction. For the PT-edge, the joint restricts the distance between the two fragments. As a result, once the carbonyls are reduced by Ca, the dangling bonds of the two reduced C atoms have more chance to bind together, owing to the high chemical activity of the dangling bonds. In this way, the reduction can proceed along the cracks and zip the two separated fragments together. Li et al.<sup>[8]</sup> suggested that the edges of graphene are the starting points for further tearing and it is easy to break the C–C bond by oxidation if the edge is broken. In this sense, cutting graphene by oxidation and zipping the GO fragments by reduction are reversible processes. Interestingly, Wang et al. suggested that metals such as Cu could be a good choice for catalyzing the cutting of carbon nanotubes into nanoribbons,<sup>[12,35]</sup> yet here, metals such as Ca with a strong reduction ability can zip GO fragments. Conversely, for the CT-edge, the Coulomb repulsion between carbonyls pushes the GO fragments away from each

other. Although Ca can randomly reduce some carbonyl groups, it becomes difficult to perfectly suture two separated GO fragments. In fact, with the periodic boundary, our PT-edge model can be considered as an edge with two closed ends. In this situation, the reduction occurs very quickly within 6 ps due to the restricted space available for the atoms. The more likely situation of a PT-edge with an open end is also considered (see Figures S2 and S3). From the results, although the reduction is slower than that of the PT-edge with two closed ends, the PT-edge with an open end may also be zipped. 2) Electronic factor: electronic structure also affects the reduction. In essence, reduction is an electron transfer from the reducing agent to oxygen, which releases the oxygen that is binding with the graphene lattice. The Fermi level of Ca is higher than that of GO.<sup>[24]</sup> Once the Ca atom moves near to the GO, the electrons on Ca transfer to the lowest unoccupied orbital of GO. Figure 4c shows the charge density of the lowest unoccupied orbital in real space for the PT-edge. The charge is mainly distributed on the unoxidized C atom with

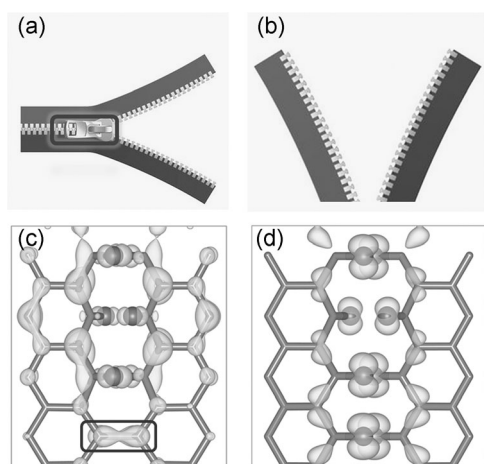


**Figure 4.** Slide fastener reduction for two GO edges: a) PT-edge with a fastener, marked by a rectangle; b) CT-edge without a fastener; c) and d) are the corresponding charge distributions of their lowest unoccupied orbitals in real space. The rectangle in (c) indicates the fastener of the GO edge. The charge isosurface value is chosen as  $0.003 e/a_0^3$ , where  $a_0$  is the Bohr radius. Color coding of atoms is the same as in Figure 1.

a delocalized orbital; thus, the Ca atom can transfer electrons to the oxidized carbon atom over a long distance along the edges. In such a case, carbonyls can be rapidly reduced by electron transfer. However, for the CT-edge, the lowest unoccupied orbital is mainly composed of the lone-pair electrons of the carbonyl and the C–C bonds near the edge. The localized orbital suppresses electron transfer from the distant Ca atom to the carbonyls, and the reduction depends on the random movement of the Ca atom close to the carbonyls.

The reduction process of the PT-edge proceeds through the following steps. First, the electrons are transferred to the unoxidized C atoms along the edges through the delocalized orbital and this weakens the C–O covalent bond. In consequence, the carbonyl oxygen atoms escape from the binding

with C with the assistance of thermal vibration, and form CaO. However, this sequential process is obstructive for the CT-edge. The localized  $\sigma$  bond along the edges prevents long-range electron transfer. The reduction depends on the random movement of Ca atoms and their approach to oxygen groups, and this makes the reduction slow and aimless. On the basis of these calculations, a zipper model may be proposed for the reduction of PT-edge, as shown in Figure 4a and c. The joint point, marked with black rectangles in Figure 4, serves as a fastener, which facilitates the reduction and zips the edges. The CT-edge, however, lacks the joint, and thus the reduction is difficult. However, considering the ideal situation, in which each of the carbonyls on the edges is removed, the two separated parts may be joined together; see Figure 5 and Figure S4. At 300 K, within just 10 fs, the distance between the two parts comes to 2.0 Å. After another 10 fs, the two parts quickly join together. With appropriate alignment and efficient reduction reagents, separated GO fragments may be integrated into a bigger graphene sheet.

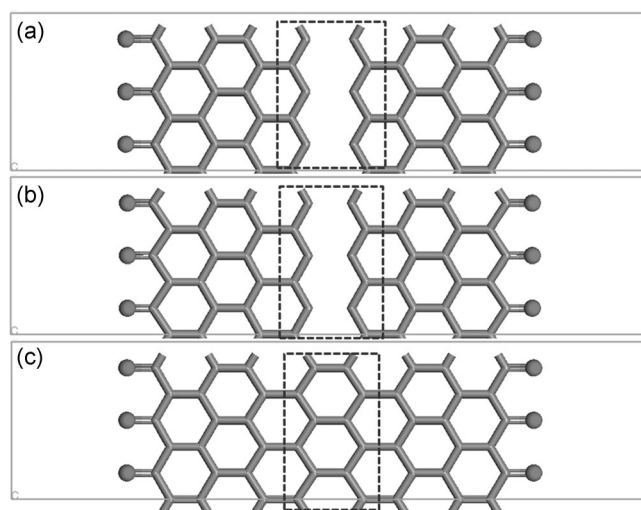


**Figure 5.** Completely reduced edges recombine automatically into entirety: a) initial model with edge separation of 2.3 Å, which is 60% larger than the standard C–C bond length in graphene; snapshots at b) 10 fs and c) 20 fs of AIMD at 300 K (the joining is finished within 20 fs). Rectangles in (a), (b), and (c) mark the edge atoms. Color coding of atoms is the same as in Figure 1.

### 3. Conclusions

Based on AIMD simulations, the reduction of GO edges by Ca metal is revealed. For a PT-edge, Ca can donate electrons to the delocalized orbital of unoxidized C atoms over a long range, and the electrons can be rapidly transferred to the oxidized C atom to make the reduction quick and effective. For a CT-edge, the lowest unoccupied orbital is localized near the edge and suppress the electron transfer to the oxidized C. As a result the reduction becomes ineffective and aimless. However, in an ideal situation, once the carbonyls are completely reduced, the two separated parts can recombine to form a bigger graphene sheet. The present work proposes a feasible method to reduce carbonyls at graphene edges by using Ca

metal. This method could zip the GO fragments produced by oxidation, and hence increase the size and improve the quality of graphene by chemical reduction, and it deserves experimental trial to produce graphene for future technological applications.<sup>[2, 4, 36]</sup>

## Acknowledgements

The present work was supported by National Natural Science Foundation of China (No. 11104109, 11374119), China Postdoctoral Science Foundation (No. 2013T60315). Also, the High Performance Computing Center (HPCC) at Jilin University is acknowledged for calculation resources. W.Q.T. thanks the Open Project of State Key laboratory of Supramolecular Structure and Materials (JLU) (SKLSSM201404).

**Keywords:** ab initio calculations · edge · electron transfer · graphene oxide · metal reduction

- [1] K. S. Novoselov, A. K. Geim, S. V. Morozov, D. Jiang, Y. Zhang, S. V. Dubonos, I. V. Grigorieva, A. A. Firsov, *Science* **2004**, *306*, 666–669.
- [2] S. Frank, *Nat. Nanotechnol.* **2010**, *5*, 487–496.
- [3] A. K. Geim, *Science* **2009**, *324*, 1530–1534.
- [4] Y.-M. Lin, C. Dimitrakopoulos, K. A. Jenkins, D. B. Farmer, H.-Y. Chiu, A. Grill, P. Avouris, *Science* **2010**, *327*, 662.
- [5] D. R. Dreyer, S. Park, C. W. Bielawski, R. S. Ruoff, *Chem. Soc. Rev.* **2010**, *39*, 228–240.
- [6] S. Pei, H.-M. Cheng, *Carbon* **2012**, *50*, 3210–3228.
- [7] J.-L. Li, K. N. Kudin, M. J. McAllister, R. K. Prud'homme, I. A. Aksay, R. Car, *Phys. Rev. Lett.* **2006**, *96*, 17610.
- [8] Z. Li, W. Zhang, Y. Luo, J. Yang, J. G. Hou, *J. Am. Chem. Soc.* **2009**, *131*, 6320–6321.
- [9] D. V. Kosynkin, A. L. Higginbotham, A. Sinitskii, J. R. Lomeda, A. Dimiev, B. K. Price, J. M. Tour, *Nature* **2009**, *458*, 872–876.
- [10] S. Fujii, T. Enoki, *J. Am. Chem. Soc.* **2010**, *132*, 10034–10041.
- [11] Y.-R. Kang, Y.-L. Li, M.-Y. Deng, *J. Mater. Chem.* **2012**, *22*, 16283–16287.
- [12] J. Wang, L. Ma, Q. Yuan, L. Zhu, F. Ding, *Angew. Chem.* **2011**, *123*, 8191–8195; *Angew. Chem. Int. Ed.* **2011**, *50*, 8041–8045.
- [13] F. Li, E. Kan, R. Lu, C. Xiao, K. Deng, H. Su, *Nanoscale* **2012**, *4*, 1254–1257.
- [14] L. Ma, J. Wang, F. Ding, *Angew. Chem.* **2012**, *124*, 1187–1190; *Angew. Chem. Int. Ed.* **2012**, *51*, 1161–1164.
- [15] M. Acik, G. Lee, C. Mattevi, M. Chhowalla, K. Cho, Y. J. Chabal, *Nat. Mater.* **2010**, *9*, 840–845.
- [16] X. Wang, L. Zhi, K. Mullen, *Nano Lett.* **2008**, *8*, 323–327.
- [17] S. Stankovich, D. A. Dikin, R. D. Piner, K. A. Kohlhaas, A. Kleinhammes, Y. Jia, Y. Wu, S. T. Nguyen, R. S. Ruoff, *Carbon* **2007**, *45*, 1558–1565.
- [18] Z.-S. Wu, W. Ren, L. Gao, B. Liu, C. Jiang, H.-M. Cheng, *Carbon* **2009**, *47*, 493–499.
- [19] H.-J. Shin, K. K. Kim, A. Benayad, S.-M. Yoon, H. K. Park, I.-S. Jung, M. H. Jin, H.-K. Jeong, J. M. Kim, J.-Y. Choi, Y. H. Lee, *Adv. Funct. Mater.* **2009**, *19*, 1987–1992.
- [20] S. Pei, J. Zhao, J. Du, W. Ren, H.-M. Cheng, *Carbon* **2010**, *48*, 4466–4474.
- [21] Y. Zhang, L. Guo, S. Wei, Y. He, H. Xia, Q. Chen, H.-B. Sun, F.-S. Xiao, *Nano Today* **2010**, *5*, 15–20.
- [22] Z.-J. Fan, W. Kai, J. Yan, T. Wei, L.-J. Zhi, J. Feng, Y.-m. Ren, L.-P. Song, F. Wei, *ACS Nano* **2011**, *5*, 191–198.
- [23] X. Mei, J. Ouyang, *Carbon* **2011**, *49*, 5389–5397.
- [24] S.-Y. Xie, X.-B. Li, Y. Y. Sun, Y.-L. Zhang, D. Han, W. Q. Tian, W.-Q. Wang, Y.-S. Zheng, S. B. Zhang, H.-B. Sun, *Carbon* **2013**, *52*, 122–127.
- [25] G. Kresse, J. Furthmüller, *Phys. Rev. B* **1996**, *54*, 11169–11186.
- [26] P. E. Blöchl, *Phys. Rev. B* **1994**, *50*, 17953–17979.
- [27] J. P. Perdew, K. Burke, M. Ernzerhof, *Phys. Rev. Lett.* **1996**, *77*, 3865–3868.
- [28] D. M. Bylander, L. Kleinman, *Phys. Rev. B* **1992**, *46*, 13756–13761.
- [29] M. C. Kim, G. S. Hwang, R. S. Ruoff, *J. Chem. Phys.* **2009**, *131*, 064704.
- [30] R. R. Lide, *CRC Handbook of Chemistry and Physics*, CRC, Boca Raton, **2000**, pp. 175–176.
- [31] A. M. Abdelkader, E. El-Kashif, *ISIJ Int.* **2007**, *47*, 25–31.
- [32] T. W. Farthing, G. Z. Chen, D. J. Fray, *Nature* **2000**, *407*, 361–364.
- [33] K. Erickson, R. Erni, Z. Lee, N. Alem, W. Gannett, A. Zettl, *Adv. Mater.* **2010**, *22*, 4467–4472.
- [34] D. Pacilé, J. C. Meyer, A. Fraile Rodríguez, M. Papagno, C. Gómez-Navarro, R. S. Sundaram, M. Burghard, K. Kern, C. Carbone, U. Kaiser, *Carbon* **2011**, *49*, 966–972.
- [35] L. Ma, J. Wang, F. Ding, *ChemPhysChem* **2013**, *14*, 47–54.
- [36] N. Papisimakis, S. Thongrattanasiri, N. I. Zheludev, F. J. García de Abajo, *Light: Sci. Appl.* **2013**, *2*, e78–e81.

Received: February 20, 2014

Revised: March 28, 2014

Published online on June 12, 2014